Chinese Journal of
POLYMER SCIENCE

RESEARCH ARTICLE

https://doi.org/10.1007/s10118-024-3068-x
Chinese J. Polym. Sci. **2024**, *42*, 322–332

Significantly Enhanced Energy Storage Performances of PEI-based Composites Utilizing Surface Functionalized ZrO_2 Nanoparticles for High-Temperature Application

Qing-Qing Liu[a,b], Qiu-Hao Lin[a,b], Xiao-Dong Qi[a,b], Nan Zhang[a,b], Ting Huang[a,b], Jing-Hui Yang[a,b*], and Yong Wang[a,b*]

[a] *School of Chemistry, Southwest Jiaotong University, Chengdu 610031, China*
[b] *Key Laboratory of Advanced Technologies of Materials, Ministry of Education of China, Southwest Jiaotong University, Chengdu 610031, China*

Electronic Supplementary Information

Abstract Polymer dielectrics with a high energy density and an available energy storage capacity have been playing an important role in advanced electronics and power systems. Nevertheless, the use of polymer dielectrics in harsh environments is limited by their low energy density at high temperatures. Herein, zirconium dioxide (ZrO_2) nanoparticles were decorated with amino group utilizing 4,4-methylenebis (phenyl isocyanate) (AMEO) and successfully incorporated into polyetherimide (PEI) matrix. The dielectric properties, breakdown strength, and energy storage performances of PEI/ZrO_2-AMEO nanocomposites were investigated from 25 °C to 150 °C. It is found that the combination of moderate bandgap ZrO_2 with modest dielectric constant and polar groups at interface with deep trap can offer an available strategy to simultaneously increase the dielectric constant and breakdown strength of polymer dielectrics. As a result, the composites containing ZrO_2-AMEO exhibit excellent energy storage performance at elevated temperatures. Specially, the PEI-based composites with 3 vol% ZrO_2-AMEO display a maximum discharged energy density (U_d) of 3.1 J/cm^3 at 150 °C, presenting 90% higher than that of neat PEI. This study may help to better develop the polymer-based dielectric composite applied at elevated temperatures.

Keywords Polyetherimide; High temperature dielectric; ZrO_2; Interface

Citation: Liu, Q. Q.; Lin, Q. H.; Qi, X. D.; Zhang, N.; Huang, T.; Yang, J. H.; Wang, Y. Significantly enhanced energy storage performances of PEI-based composites utilizing surface functionalized ZrO_2 nanoparticles for high-temperature application. *Chinese J. Polym. Sci.* **2024**, *42*, 322–332.

INTRODUCTION

Dielectric capacitors are of great significance for integrated electronics and electrical system owing to their application in power conversion, energy storage, *etc*.[1–4] Polymer-based composites are the preferable materials for capacitors due to the high breakdown strength, flexibility, cost-effective manufacture, and ease of processing compared to traditional ceramic dielectrics.[5–7] There has been extensive research into polymer-based dielectric composites nowadays, and it has been realized that the shortcomings of low dielectric constant and low thermal stability of polymers need to be overcome. For example, even though the latest commercially available biaxially orientated polypropylene (BOPP) film exhibits a high breakdown strength of ~700 MV/m, the maximum operating temperature of BOPP cannot exceed 105 °C. Meanwhile, its breakdown strength, charge-discharge efficiency and mechanical properties could be sharply deteriorated as the temperature rises above 70 °C.[8] However, the technologies and emergent industries, such as hybrid electric vehicles (HEV), aerospace engineering and oil exploration, *etc*., have put forwards more severe requirements for operating temperatures.[9–11] The operating temperature of the capacitors in HEVs is 250 °C, which is even higher than that of underground oil exploration. Therefore, the polymer-based dielectric cannot meet the industrial requirement at high temperature. It is such clear that the new generation of dielectric capacitors with high operating temperature and favorable dielectric properties is in urgent need.

To address the urgent requirements, some high glass transition temperature (T_g) engineering polymers, such as polyphenylene sulfide (PPS), poly(acylene ether urea) (PEEU), polyimide (PI) and polyacrylonitrile (PAN), *etc*., are utilized as polymer dielectric materials for high temperature application. However, it is well recognized that engineering polymers with excellent thermal stability are able to performance well at harsh temperature but only at low electrical fields. Owing to the thermal/electrical field charge injection, excitation, and transport, the combination of harsh temperature and high voltage significantly reduces the dielectric loss and energy storage capacity of polymers.[12] On the other hand, it is widely recognized that the capacitive energy density (U_e) of di-

* Corresponding authors, E-mail: yangjinghui_84@163.com (J.H.Y.)
E-mail: yongwang1976@swjtu.edu.cn (Y.W.)

Received September 1, 2023; Accepted November 9, 2023; Published online December 7, 2023

electrics are decided by the equation as $U_e = \frac{1}{2}\varepsilon_0\varepsilon_r E^2$ (ε_0 is the vacuum dielectric constant), but simultaneously improving dielectric constant (ε_r) and breakdown strength (E_b) for polymer dielectrics still remains difficult. One approach to meeting the pressing need for high-temperature polymer film dielectric capacitors is chemical crosslinking. This involves covalently linking polymer chains to form a chain network structure. The movement of the polymer chains can be effectively restricted by the cross-linked structure, resulting in the reduction of dielectric loss and increment of E_b at high temperature. The other one is to construct layered structures in polymer dielectric composites, in which the upper layer of polymer thin films was often coated by an inorganic layer to raise the energy barrier at the electrode/dielectric interface, thereby eliminating the Schottky emission conduction current.[13] However, the process of cross-linking and constructing layered polymers are of complexity and comparatively high-cost, limiting its salable production.

Recently, inorganic fillers have been incorporated into high T_g polymer dielectrics to fabricate the organic-inorganic polymer-based composite dielectrics, in which the advantages of flexible polymer matrix and inorganic fillers are expected to be retained. Specially, the introduction of wide bandgap (E_g) inorganic fillers, such as silica (SiO_2), magnesium oxide (MgO), boron nitride nanosheet (BNNS), *etc*., have been proven to benefit the reduction of conduction loss under high field and high temperature.[14–16] It is well recognized that the inorganic fillers with higher E_g are beneficial for capturing the carriers or space charges *via* providing deep trap in the polymer composites. At the same time, the polymer composites containing inorganic filler with high E_g usually exhibit modest improvement on the dielectric constant due to the limited polarization capacity under electric field. For example, the BNNS/ polyetherimide (PEI) composites exhibit a slight increase in dielectric constant, from 3.26 for pure PEI to 3.42 of the composites containing 7 vol% BNNS.[17] In this case, the investigation on fillers with moderate bandgap has greatly attracted great attentions, which has been regarded to be of great importance for avoiding electric field distortion and overcoming the high dielectric loss at high electric field and harsh temperature.[18] The inorganic filler such as zirconium dioxide [ZrO_2 (ε_r~25, E_g~6 eV)] and hafnium oxide [HfO_2, (ε_r~25, E_g~5.8 eV)] with moderate bandgap have been proven to be positive on the dielectric capacitor for high temperature application.[19,20] Zheng *et al*. developed a P(VDF-HFP) composites embedded with ZrO_2 as core and coated by Al_2O_3, which exhibited improved capacitive performances. The resulting composites possess superior ability to prevent charge movement due to the increased activation energy of two interfacial polarization, leading to enhanced dielectric and energy storage properties.[21] Meanwhile, Ren *et al*. utilized ZrO_2 and Al_2O_3 particles to construct a ZrO_2@Al_2O_3 core-shell particles and the incorporated the particles into PEI matrix. In this case, much less distorted electric field, and high breakdown strength over a range of temperatures has been achieved by creating a gradient of dielectric constant between ZrO_2 and Al_2O_3. Owing to the optimized structure, the composite exhibits high energy density and charge-discharge efficiency.[22] On the other hand, it is well documented that the effect of nanoparticles is dependent on the interface adhesion between nanoparticles and polymer matrix. Therefore, interfacial modification on the nanoparticles has been widely applied to improve the interfacial interaction between inorganic fillers and polymer matrix. However, it is still a lack of reports on the effect of interfacial modification on high-temperature dielectric capacitors. Li *et al*. mentioned that for purpose of satisfying the requirement of dielectric capacitors, not only the compatibility between modified particles and polymers should be considered, but also it is necessary to consider the regulation of dielectric properties by surface engineering.[23] They found that a polypropylene-graft-maleic anhydride (PP-*g*-MAH) coating on magnesium oxide (MgO) showed adequate compatibility with the polypropylene (PP) matrix, resulting in the suppression of electrical conduction *via* providing deep energy traps from MAH and benefiting the improved dielectric constant thanks to the polar molecular element. Despite the important role of interfaces has been widely acknowledged, few studies have focused directly on interfacial modification through interfacial engineering for high-temperature application.

PEI is one kind of linear polymers with high T_g (~215 °C) and excellent E_b, which are beneficial for its applications under high-temperature environments.[24–26] In this work, the ZrO_2 particles with moderate bandgap (E_g~6 eV) and dielectric constant (25) are applied as dielectric filler to enhance the dielectric property of PEI. Firstly, ZrO_2 nanoparticles are functionalized with a layer of 4,4-methylenebis (phenyl isocyanate) (AMEO), which is expected to not only show improved compatibility between ZrO_2 nanoparticles and PEI matrix but also to offer energy traps *via* introducing amino group. Herein, the composites exhibit maximum U_e of 3.1 J/cm^3 and charge-discharge efficiency of 60% at 150 °C. We not only interpret the interface chemical structure and its resultant effects on chain movement at interface, but also try to establish the correlations among deep trap of amino groups, intrinsic characteristics of ZrO_2, and macroscopic dielectric property at high temperature. The aim of this work is to enrich the understanding on interface modification of particles in polymer-based dielectric composites and explore the new method for developing high-temperature dielectric polymer composites.

EXPERIMENTAL

Materials

ZrO_2 nanoparticles (3 g, average particle size less than 100 nm, Shanghai Aladdin Reagent) were dispersed into 150 mL of ethanol (Chengdu Kelong Chemical Co., Ltd.) and sonicated for 20 min, then 3 mL of AMEO (MDI, 98%, Shanghai Aladdin Reagent) was added. And then the solution was mechanically stirred at 80 °C and condensed under reflux for 24 h. After centrifugation at 6000 r/min for 5 min, the solution was washed and rinsed with ethanol then dried in a vacuum oven at 80 °C for 10 h. The modified ZrO_2 was acquired and named as ZrO_2-AMEO.

Preparation of ZrO_2-AMEO/PEI Composites Films

At first, a certain amount of ZrO_2-AMEO filler was dispersed into *N*-methyl-2-pyrrolidone (NMP, Chengdu Kelong Chemical Co., Ltd.) and sonicated for 1 h. Secondly, corresponding PEI (Ultem 1000, SABIC Innovative Plastics) was added to the ZrO_2-

https://doi.org/10.1007/s10118-024-3068-x

AMEO/NMP mixed solution, and the mixture was stirred at 80 °C for 5 h and 20 °C for 10 h, respectively, to acquire a uniformly dispersed solution. After defoaming in vacuum, the solution was smoothly scraped on the glass substrate by a scraper with a specification of 150 μm. The films were then dried at 60 °C for 24 h for solvent removal. Lastly, the resulting film was stripped from the substrate and then dried at 120 °C for 12 h to remove residual solvent thoroughly. The typical thickness of the composite films was approximately 16 μm. Inside the ZrO_2-AMEO/PEI composites, the volume fraction of ZrO_2-AMEO nanoparticles was 1 vol%, 3 vol%, and 5 vol%, respectively. Pure PEI and ZrO_2 /PEI composite films were also prepared in the same route. The schematic fabrication processes of the ZrO_2-AMEO/PEI composites films are displayed in Fig. 1.

Characterization

The morphology of AMEO-modified ZrO_2 was observed *via* a transmission electron microscope (TEM, JEOL 2100F, Japan) with an accelerating voltage of 200 kV. Thermogravimetric analysis (TGA, TG 209 F1 Libra®, NETZSCH, Germany) was carried out under nitrogen atmosphere with the temperature range of 25-800 °C at the heating rate of 10 °C/min. A Fourier transform infrared (FTIR) spectrometer (Nicolet IS10, Thermo Fisher Scientific Inc., USA) was used to determine the chemical composition of ZrO_2 and ZrO_2-AMEO at a resolution of 4 cm^{-1} over a range of 4000–500 cm^{-1} *via* transmission mode. The surface elements and chemical composition of ZrO_2-AMEO were characterized using an X-ray photoelectron spectrometer (XPS, Thermo Scientific K-Alpha, USA) with 12 kV working voltage and 6 mA current via monochromatic Al K*α* X-ray source with 1486.6 eV photons. The cross-sectional morphology of PEI/ZrO_2-AMEO composite film was observed by a scanning electron microscope (SEM) Fei Inspect (the Netherlands). To determine the dispersion state of ZrO_2 in polymer matrix, the composites were pre-cooled in liquid nitrogen for 20 min to obtain the fractured surfaces for observation. The accelerating voltage for the SEM characterization was 20 kV, and all samples were sprayed with gold to improve electrical conductivity. The dielectric constant and loss tangent was tested by a Concept 50 broadband dielectric spectrometer (Novocontrol, Germany). The spectrometer was operated at 20 V in the frequency range 10^2–10^6 Hz. A breakdown voltage tester (BDJC-50, Beiguang Jingyi Instrument) was used to test the breakdown strength. The temperature range was tested from 25 °C to 150 °C. A ferroelectric test system (TF 2000E, aixACCT, Germany) was used to measure the dynamic hysteresis loops at a frequency of 100 Hz. For dielectric measurements, the 4 mm diameter gold electrodes were sputtered on two sides of the composite films.

RESULTS AND DISCUSSION

Microstructure of ZrO_2-AMEO and PEI Composites

Firstly, the chemical composition of modified ZrO_2 was investigated. Fig. 2(a) presents the FTIR spectra of neat ZrO_2 and AMEO modified ZrO_2 nanoparticles (ZrO_2-AMEO). The absorbance bands of ZrO_2 and ZrO_2-AMEO nanoparticles at 3340 and 1632 cm^{-1} are assigned to the stretching vibrations of O—H bonding and C—OH bonding. The band at 747 cm^{-1} for both ZrO_2 and ZrO_2-AMEO nanoparticles is attributed to the characteristic vibration band of Zr-O. Two new absorbance bands at 2924 and 2855 cm^{-1} appear for the AMEO modified ZrO_2, which are originated from the stretching vibration of $-CH_3$ and $-CH_2$ in the chain skeleton of AMEO. Another characteristic band at 1022 cm^{-1} for ZrO_2-AMEO is assigned to the stretching vibration of Si—O—Si.[27,28] Fig. 2(b) shows the TGA curves of ZrO_2 and ZrO_2-AMEO heating from room temperatures to 800 °C in nitrogen atmosphere. It can be found that the maximum mass loss occurs at 200–400 °C for both of ZrO_2 and ZrO_2-AMEO, corresponding to the loss of most of the oxygen-containing groups and the silane chain, respectively. Compared with ZrO_2, the mass loss of ZrO_2-AMEO exhibits slightly increase, suggesting the presence of AMEO indirectly. The chemical composition of the ZrO_2 and ZrO_2-AMEO were further explored *via* XPS as demonstrated in Figs. 2(c) and 2(d). As observed from the full

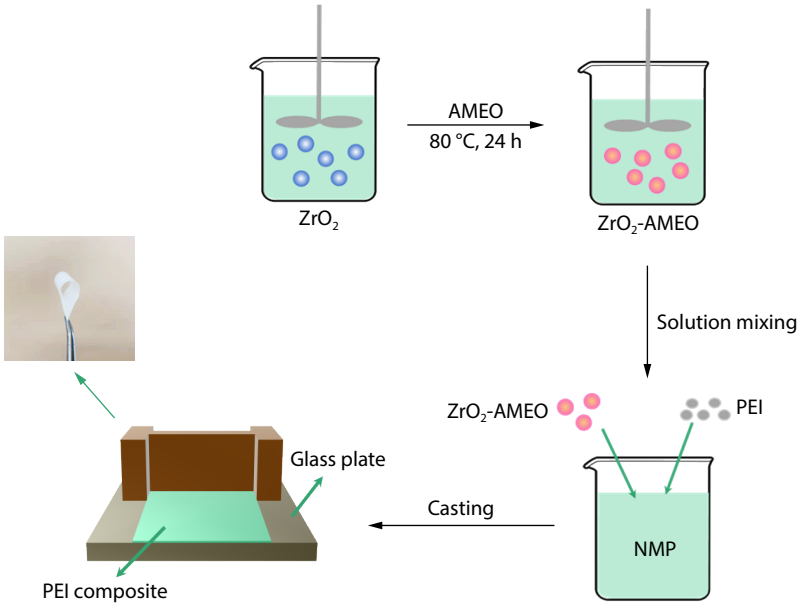

Fig. 1 Schematic diagrams of the fabrication procedures of ZrO_2-AMEO/PEI composite films.

https://doi.org/10.1007/s10118-024-3068-x

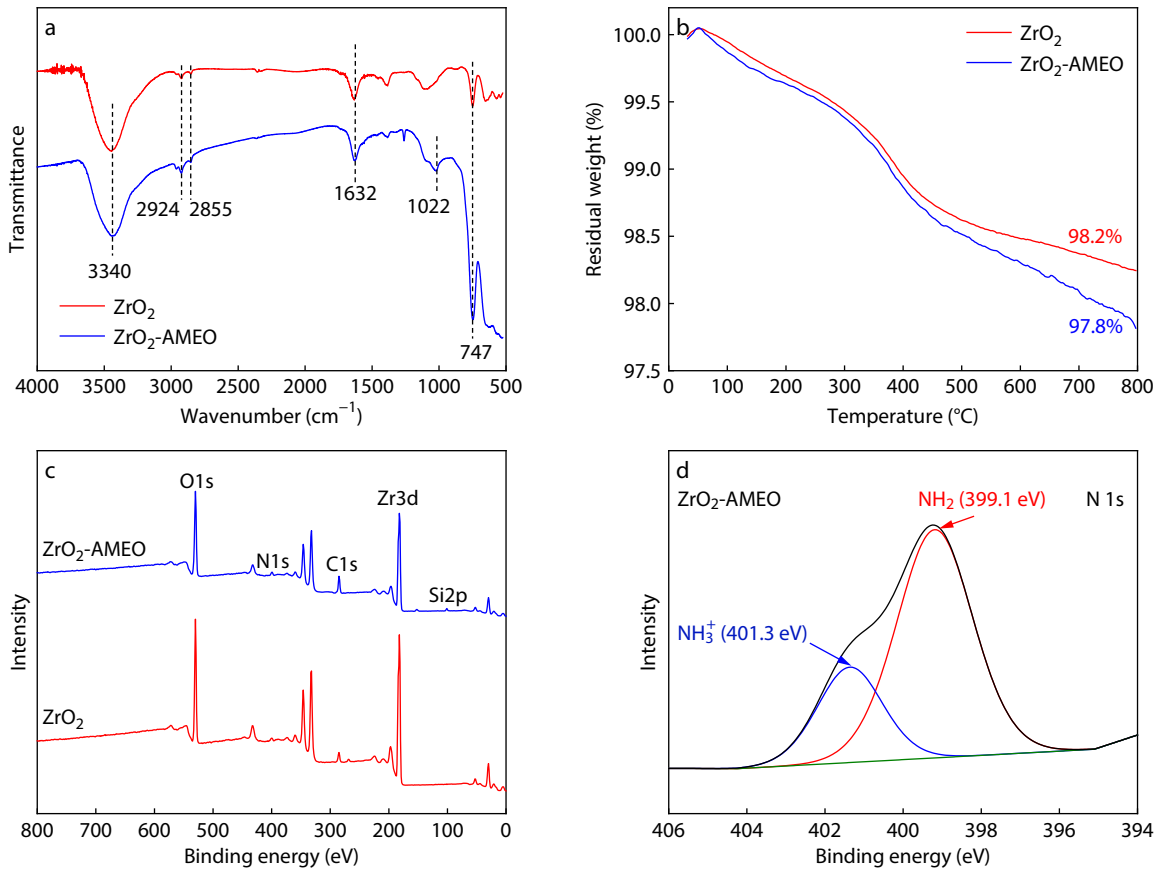

Fig. 2 (a) FTIR spectra of ZrO_2, ZrO_2-AMEO fillers in 4000–500 cm^{-1}; (b) TGA curves of ZrO_2 and ZrO_2-AMEO fillers; (c) Comparison of XPS spectra between ZrO_2 and ZrO_2-AMEO fillers; (d) The N 1s XPS spectra of ZrO_2-AMEO fillers.

spectra in Fig. 2(c), ZrO_2 exhibits the peaks of Zr 3d (182.3 eV) and O 1s (530.0 eV). The new N 1s and Si 2p peaks in the ZrO_2-AMEO derive from the introduction of polar nitrogen-containing groups and silane chains of AMEO. Specially, the N 1s peak for ZrO_2-AMEO nanoparticles can be divided into two peaks at 401.3 and 399.1 eV as shown in Fig. 2(d), which correspond to NH_3^+ and free $-NH_2$, respectively.[29,30] All these results about the chemical composition indicate that the ZrO_2 nanoparticles were successfully modified by AMEO.

The surface modification of ZrO_2 also was directly observed by TEM characterization. As shown in Fig. 3(a), the ZrO_2 nanoparticles exhibit an average diameter of ~30 nm and the surface of ZrO_2 is smooth as shown in the enlarged picture of Fig. 3(b). After being functionalized by AMEO, the morphology of ZrO_2-AMEO is retained as shown in Fig. 3(c), but the surface of ZrO_2 became rough and a layer coated of AMEO on ZrO_2 surface with 2 nm thickness can be observed from Fig. 3(d).

Fig. 4 shows the cross-sectional SEM images of ZrO_2/PEI and ZrO_2-AMEO/PEI composites with the filler loading of 1 vol% and 5 vol%, respectively. The cross-sectional SEM images exhibit smooth surface and voids/defects-free quality inside the composites containing ZrO_2 and ZrO_2-AMEO. With the low loading 1 vol% of nanoparticles, the as-received ZrO_2 (Figs. 4a and 4a′) and ZrO_2-AMEO (Figs. 4c and 4c′) nanoparticles were greatly dispersed in the PEI. With the increasing loading of particles to 5 vol%, a few ZrO_2 aggregates are observed as indicated by the arrow shown in Figs. 4(b) and 4(b′). Due to hydrogen bonding, the AEMO-modified ZrO_2 nanoparticles are still uniformly dispersed in the PEI matrix. between polar groups $-NH_2$ in AMEO with $-C=O$ of PEI (Figs. 4d and 4d′).[31] This interfacial interaction can not only effectively improve the compatibility between ZrO_2 and PEI matrix, but also help to withstand high voltage *via* avoiding

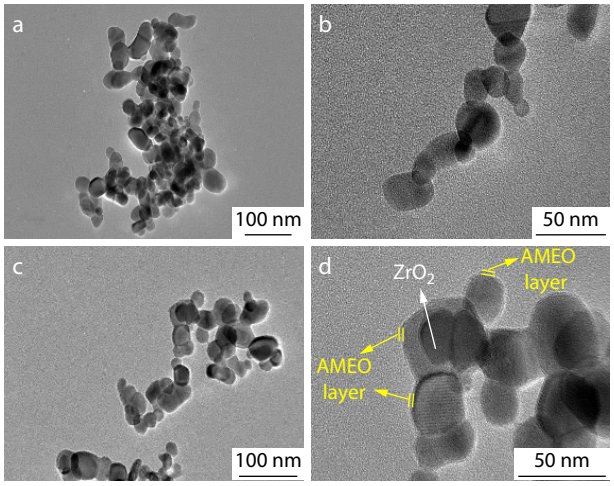

Fig. 3 TEM images of ZrO_2 at (a) low magnification and (b) high magnification; TEM images of ZrO_2-AMEO at (c) low magnification and (d) high magnification.

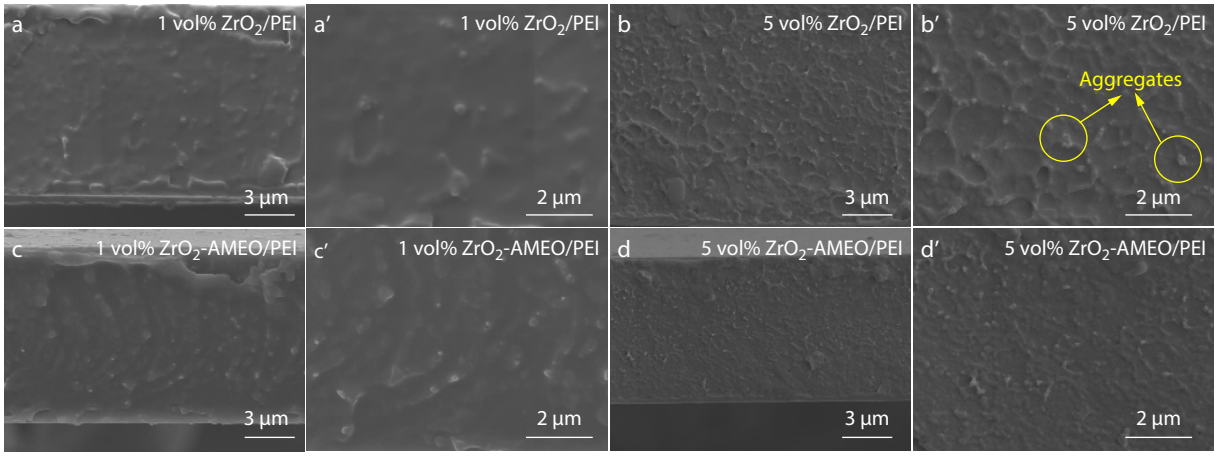

Fig. 4 SEM images of (a, a′) 1 vol% ZrO_2/PEI and (b, b′) 5 vol% ZrO_2/PEI composites, (c, c′) 1 vol% ZrO_2-AMEO/PEI and (d, d′) 5 vol% ZrO_2-AMEO/PEI composites.

the interfacial defects or voids. On the other hand, the improved compatibility between ZrO_2 and PEI matrix can benefit the dispersion, resulting in enhancement of interfacial polarization.

Dielectric Property of Composites

The dielectric constant and the loss tangent of the PEI, ZrO_2/PEI and ZrO_2-AMEO/PEI at room temperature (25 °C) are illustrated in Figs. 5(a) and 5(b). The neat PEI and PEI-based composites, the dielectric constant is stable within the frequency range of 10^2–10^6 Hz. And the dielectric constant of PEI-based films rises as the loading of nanoparticles increases. For example, as shown in Fig. 5(a), the dielectric constant of pure PEI is 4.4@1 kHz, and the dielectric constant reaches up to 6.0@1 kHz and 7.1@1 kHz for the composites containing 1 vol% and 3 vol% ZrO_2, respectively. The improvement of dielectric constant is mainly originated from the intrinsic dipole polarization of ZrO_2 and interfacial polarization. Specially, when the loading of ZrO_2 increases to 5 vol%, the dielectric constant decreases with increasing the frequency at high frequency region of 10^2–10^3 Hz, which indicates that as the nanoparticle loading increases, the interfacial polarization becomes dominant in the composites. Meanwhile, the dielectric loss remains below 0.0075, although the dielectric loss of composites containing 5 vol% ZrO_2 exhibits sharply increase to 0.015@1 kHz owing to the enhanced interfacial polarization. The incorporation of ZrO_2-AMEO further improves the dielectric constant. At the loading of 5 vol%, the dielectric constant of ZrO_2/PEI composite is 7.5@1 kHz while the dielectric constant of ZrO_2-AMEO/PEI composite is elevated to 8.5@1 kHz (Fig. 5b). This can be attributed to the improved dispersion of ZrO_2-AMEO in PEI matrix due to the enhanced interfacial interaction. Correspondingly, the dielectric loss of composites containing ZrO_2-AMEO has little change in comparison to the composites containing ZrO_2. Concurrently, it is found that the polarization of the composites is unable to follow the rapid alternation of electric field, leading to the high polarization loss at high frequency.[13] Fig. S1 (in the electronic supplementary information, ESI) illustrated the alternating current (AC) conductivity of the PEI composites as a function of frequency. The AC conductivity of all PEI-based composite is strongly dependent on the frequency. At 10^3 Hz, the conductivity of the composite materials is kept at a low level of around 10^{-12}–10^{-10} S/cm, indicating that all that PEI-based composites are insulating and well below the percolation threshold. Thus, they are capable of being used as dielectric composites.

Furthermore, Fig. 6 exhibits the dielectric stability of PEI,

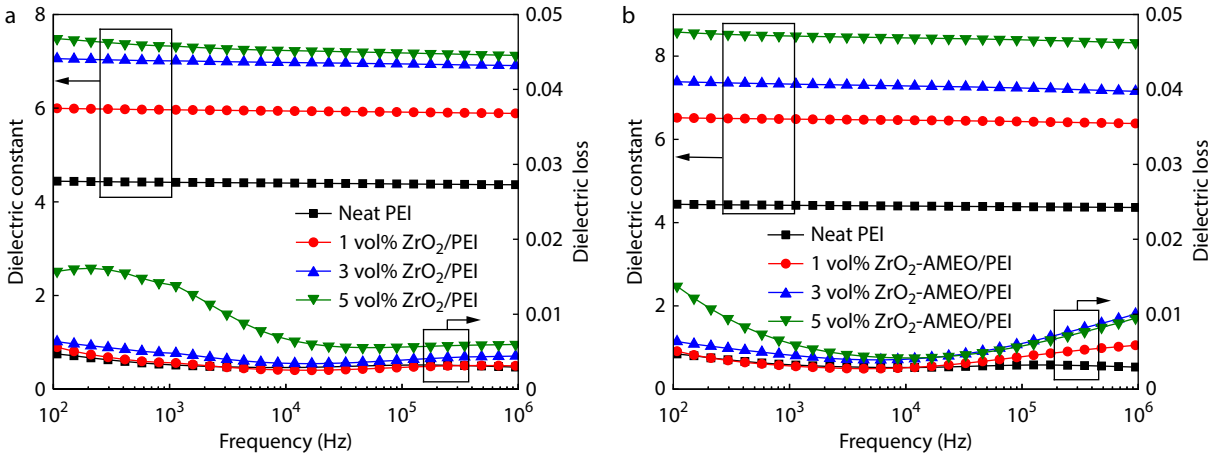

Fig. 5 Dielectric constant and dielectric loss of the PEI composite materials with different filler contents at 25 °C: (a) ZrO_2/PEI, (b) ZrO_2-AMEO/PEI.

https://doi.org/10.1007/s10118-024-3068-x

ZrO_2/PEI composites and ZrO_2-AMEO/PEI composite films under the temperature range of 25–150 °C, respectively. The dielectric constant of ZrO_2/PEI and ZrO_2-AMEO/PEI exhibits good thermal stability over the wide temperature range from 25–150 °C. It is noted that the dielectric loss of all the composites remains below 0.03 within the temperature range, which can be ascribed to the carrier capture of moderate bandgap of ZrO_2. Owing to the participation of thermal free charge carriers into the conduction process at high temperature, the dielectric loss of pure PEI exhibits a gradual increase at 100–150 °C. However, the incorporation of ZrO_2 is beneficial for further suppressing the dielectric loss owing to the carrier capture of ZrO_2 and the dielectric loss exhibits tiny fluctuation for composites containing ZrO_2 and ZrO_2-AMEO within a wide temperature range. Furthermore, the interface modified ZrO_2 *via* AEMO is helpful for further decreasing the dielectric loss. As it is shown, the dielectric loss of PEI composites containing ZrO_2-AMEO is lower than that of composites containing the same loading of ZrO_2. At the same time, the rise of dielectric loss for ZrO_2/PEI composites starts from 125 °C whereas the loss of ZrO_2-AMEO/PEI composites exhibits an increase when the temperature rises to 130 °C. All the results indicate that the incorporation of AMEO plays a positive role on suppressing the dielectric loss at high temperature.

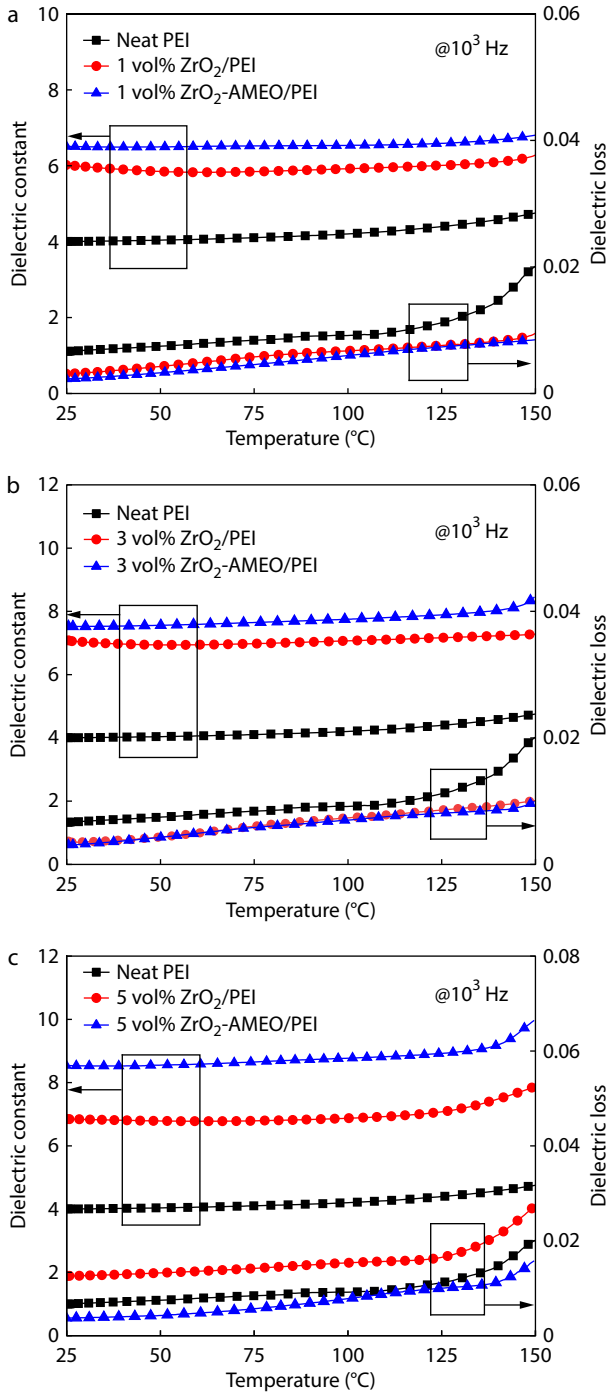

Fig. 6 Temperature-dependent dielectric spectra of PEI, the PEI/ZrO_2, and PEI/ZrO_2-AMEO nanocomposites at 1 kHz with varied filler loadings: (a) 1 vol%, (b) 3 vol%, and (c) 5 vol%.

In addition, E_b is also a decisive parameter for the energy storage density. The Weibull distribution function was used for the calculation of the breakdown strength of the composites with ZrO_2 and ZrO_2-AMEO, in accordance with the following equation:[32]

$$P(E) = 1 - \exp\left[-\left(\frac{E}{E_b}\right)^{\beta}\right] \quad (1)$$

where $P(E)$ represents the cumulative probability of electric failure, E is the experimental breakdown strength, and E_b is the characteristic breakdown strength which is referred to the cumulative failure probability reach 63.2%, and shape parameter β reflects the scatter degree of the experimental data. The Weibull-distribution graph and the corresponding characteristic breakdown strength of the composites with ZrO_2 and ZrO_2-AMEO fillers under different filler loadings are shown in Figs. 7(a) and 7(b). With the increase of filler loading, the E_b of the composites exhibits a first increasing and then decreases at the loading of 5 vol%, and the composites containing 3 vol% ZrO_2-AMEO represent the largest E_b of 404.8 MV/m, exhibiting 27% higher than that of neat PEI. On one hand, the dielectric constant of ZrO_2 is 25, near to that of neat PVDF. This could avoid interface electric field distortion to some extent, leading to enhancement in withstanding the electric breakdown. On the other hand, the ZrO_2-AMEO nanoparticles are uniformly dispersed in the PEI and have better interfacial interactions with the matrix, thus reducing the irregular distribution of the electric field in the composites and improving the breakdown strength. In this case, even though at high loading of 5 vol%, the E_b of ZrO_2-AMEO/PEI composite can reach up to 302. 9 MV/m, 31.3% higher than that of composites containing the same loading of ZrO_2 nanoparticles.

To further assess the energy storage performance of PEI-based composites, unipolar *P-E* loops under different temperature at 25, 100 and 150 °C were recorded, which are shown in Fig. S2, Fig. S3 and Fig. S4 (in ESI), respectively. Firstly, the electric displacements (D) are gradually improved with the increasing loading of nanoparticles, exhibiting the linear relationship with dielectric constant. Secondly, the energy storage behaviors of pure PEI and PEI-based composite films at elevated temperatures are summarized in Fig. 8. It can be found that at room temperature, the introduction of ZrO_2 into the PEI matrix yields increments of discharged energy density (U_d) compared with neat PEI at the same electric field, which is

https://doi.org/10.1007/s10118-024-3068-x

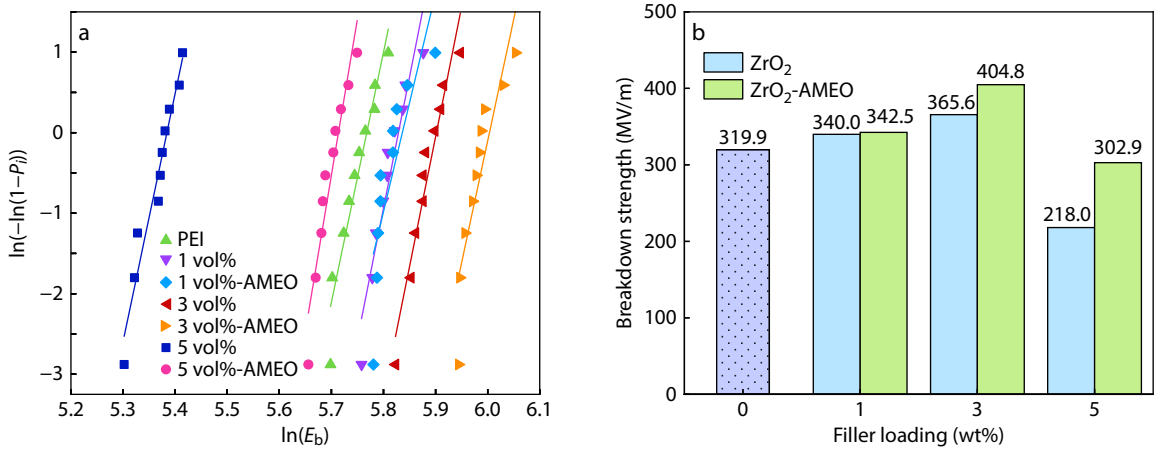

Fig. 7 (a) Weibull distribution and (b) the comparison of Weibull breakdown strength of neat PEI and composites with ZrO_2 and ZrO_2-AMEO fillers under different filler loadings.

owing to the enhanced polarization from the intrinsic dipole polarization of ZrO_2 and interface. However, higher loading of ZrO_2 results in lower charge-discharge efficiency (η). The U_d of PEI is only 3.2 J/cm^3 at 375 MV/m and the corresponding η is 77%. As for the ZrO_2/PEI composites, the U_d can rise to 5.21 J/cm^3 at 425 MV/m and the η decreases to 59% when the ZrO_2 loading is 1 vol% (Fig. 8a). ZrO_2-AMEO nanoparticles exhibit more effective effects on enhancing the energy storage, and the maximum U_d of PEI-based composites can reach up to 6.48 J/cm^3 at 425 MV/m when the ZrO_2-AMEO loading is increased to 3 vol% (Fig. 8b). Obviously, the significant increase of U_d in the ZrO_2-AMEO/PEI composite can be ascribed to the elevated E_b and polarization capacity.

Under high temperature (100 and 150 °C), as shown in Figs. 8(c)–8(f), the η of neat PEI decreases rapidly with the rising electric field, for example, at 200 MV/m and 100 °C, the η is below 70% and the U_d is only 1.0 J/cm^3. Under the same condition, a higher U_d and η can be achieved for the ZrO_2/PEI composites, and a maximum U_d of 1.2 J/cm^3 accompanied with η of 84% are obtained for the composites containing 3 vol% ZrO_2 particles. A further elevation of U_d and η can be found for ZrO_2-AMEO/PEI composites and the U_d of ZrO_2-AMEO/PEI composites has a maximum value of 1.4 J/cm^3 accompanied with η of 80% (Fig. 8d).

Fig. 9 demonstrates the maximum U_d and corresponding η as a function of temperature. It can be found that the maximum U_d declines consistently with temperature owing to the intense increase in electrical conduction with the temperature at high electric fields. The maximum U_d of neat PEI is reduced from 3.5 J/cm^3 at 25 °C to 0.3 J/cm^3 at 150 °C. For all the composites, the U_d of the composites are found to be maximized at 3 vol% nanoparticles. The composites containing 3 vol% ZrO_2 exhibit the U_d of 3.4, 2.5 and 0.8 J/cm^3 with the temperature increases from 25 °C to 100 °C and 150 °C, respectively. The PEI composites filled with 3 vol% ZrO_2-AMEO nanoparticles promote the U_d to 6.2, 3.2 and 3.0 J/cm^3 at 25, 100 and 150 °C, which are 43.5%, 60% and 90% higher than that of neat PEI, respectively. Correspondingly, the η of PEI containing 3 vol% ZrO_2-AMEO nanoparticles is as high as 64%. Obviously, the AMEO modified ZrO_2 nanoparticles exhibit more excellent energy storage performances, involving higher discharge energy density, greater power density, faster discharge rate and better thermal stability under high temperature.

To understand the excellent energy storage performance of the ZrO_2-AMEO/PEI composites, the interfacial structure is deemed to be one important issue. Based on the classical model of multi-core, the interface can provide charge traps, leading to the scattering of carriers or suppressing the carrier mobility *via* trapping. In this study, the bandgap of PEI matrix is 3.2 eV while the bandgap of ZrO_2 is 6 eV, the difference in bandgap makes it possible that the interface can effectively capture carriers or eliminate the charge density. On the other hand, amino groups in the AMEO are also recognized as a deep trap, which further enhance the capability of suppressing the charge density. These issues are important for the decreasing of dielectric loss and elevation of energy storage. Furthermore, to rationalize the effect at high temperature, the interfacial interaction and the corresponding leakage current have been examined *via* FTIR and current density measurement, respectively. Fig. 10(a) shows the FTIR spectra of neat PEI, ZrO_2/PEI and ZrO_2-AMEO/PEI. Obviously, PEI, ZrO_2/PEI and ZrO_2-AMEO/PEI composites all show the identical band at 1211 cm^{-1}, corresponding to the stretching vibration band of C—N on the PEI chain. Moreover, the red shift of C=O band from 1716 cm^{-1} of PEI and ZrO_2/PEI composite to 1712 cm^{-1} of ZrO_2-AMEO/PEI composite appears in the Fig. 10(a), which indicates that hydrogen bonding is formed between NH_2 in silane coupling agent and C=O in PEI, thus generating strong intermolecular interaction between ZrO_2-AMEO and PEI. The formation of intermolecular interaction can restrain the relaxation of PEI chains at interface, suggesting that it is not easy for the trapped carriers to escape or move up through chain mobility at high temperature. Fig. 10(b) illustrates the leakage current density of neat PEI, 3 vol% ZrO_2/PEI and 3 vol% ZrO_2-AMEO/PEI composites at 100 °C. It is obvious that the neat PEI possesses the largest leakage current, while the leakage current density of 3 vol% ZrO_2 AMEO/PEI composites is the lowest. Under the electric field of 100 MV/m, the leakage current density of PEI, 3 vol% ZrO_2/PEI and 3 vol% ZrO_2-AMEO/PEI composites are 5.94×10^{-7}, 4.82×10^{-7} and 2.66×10^{-7} A/cm^2, respectively. Based on these results, the

https://doi.org/10.1007/s10118-024-3068-x

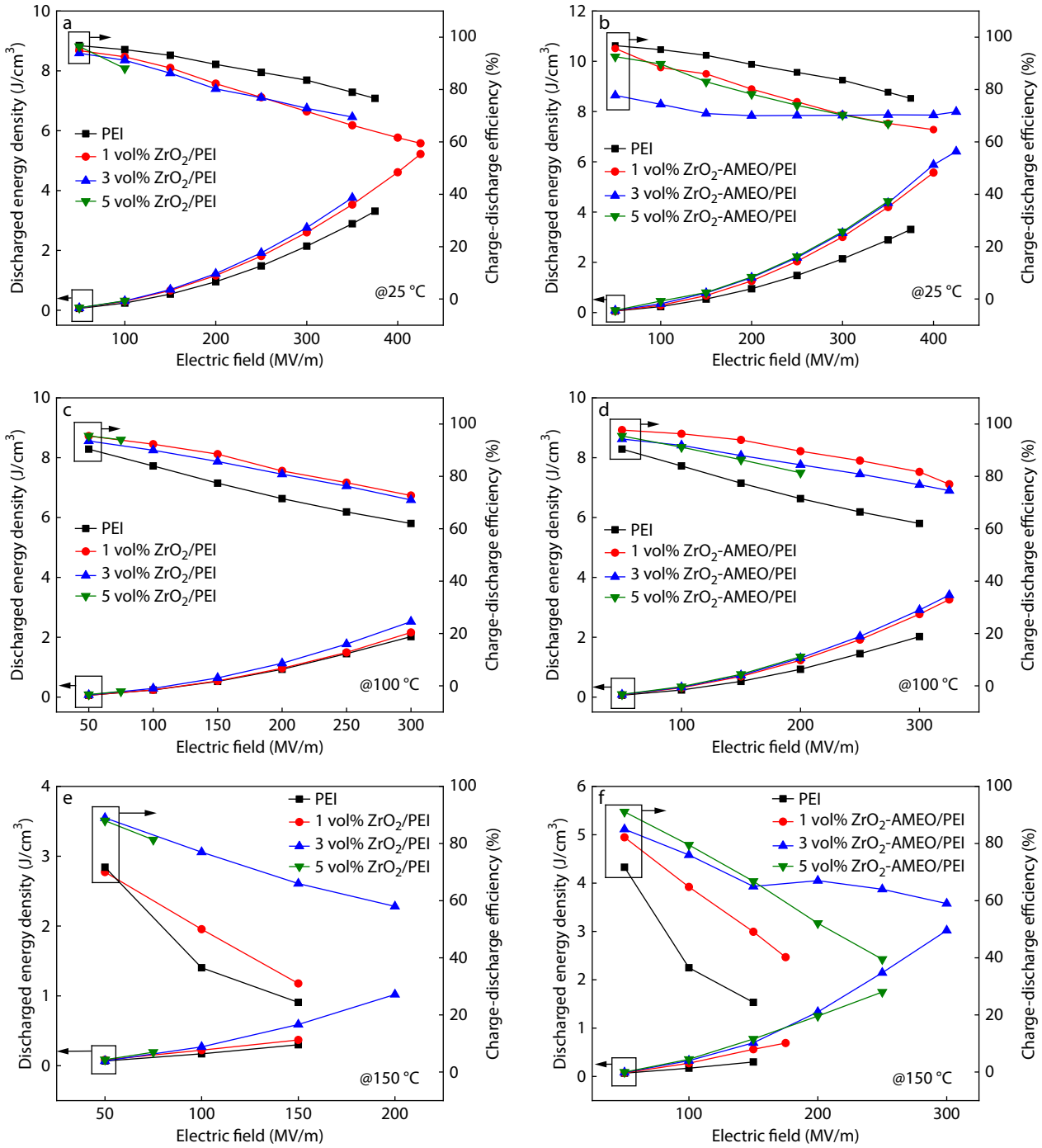

Fig. 8 The discharge energy density and charge-discharge efficiency of ZrO_2/PEI and ZrO_2-AMEO/PEI composites tested at the temperature of (a, b) 25 °C, (c, d) 100 °C and (e, f) 150 °C.

schematic picture for the underlying mechanism of neat PEI and the ZrO_2-AMEO/PEI nanocomposite are proposed as shown in Figs. 10(c)–10(d). At low temperature and low electric field, different from pure PEI, the incorporation of the moderate bandgap ZrO_2 fillers is conducive to efficiently reduce the current density of PEI under the same electric field, while the ZrO_2-AMEO can further eliminate the current density.[33] AMEO can improve the dispersion of ZrO_2 and interfacial polarization as an interface layer in composites, leading to higher storage density of ZrO_2-AMEO/PEI composite. Meanwhile, AMEO and ZrO_2 can cooperate to form deep traps to capture carriers under harsh temperature circumstance, further diminishing the generation of internal leakage current of the composite and conductivity loss, which is conducive to improve charge-discharge efficiency of the composite. Furthermore, the interfacial interaction further suppresses the chain relaxation at interface, exerting the potential of ZrO_2-AMEO to hinder or prevent the transport of charge carriers

https://doi.org/10.1007/s10118-024-3068-x

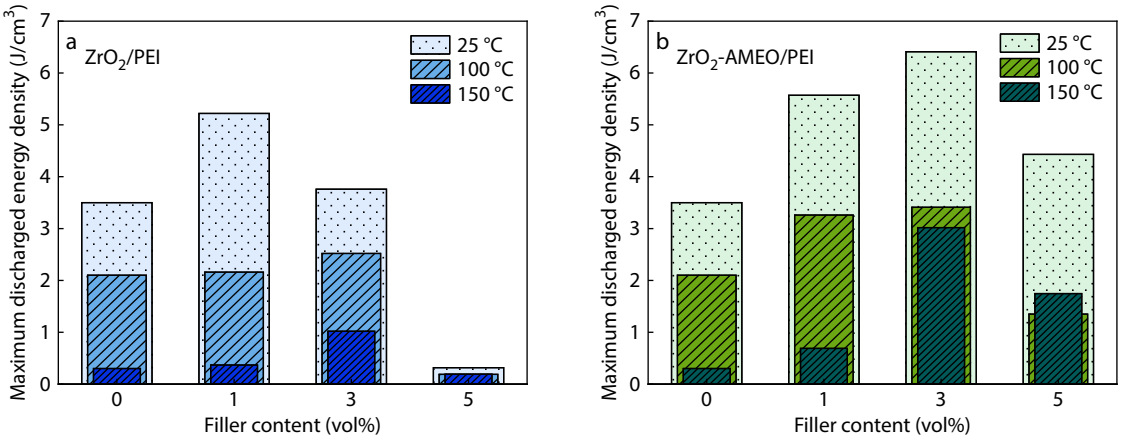

Fig. 9 Maximum discharged energy density of the (a) ZrO_2/PEI; (b) ZrO_2-AMEO/PEI composites as a function of the filler loadings at 25, 100 and 150 °C.

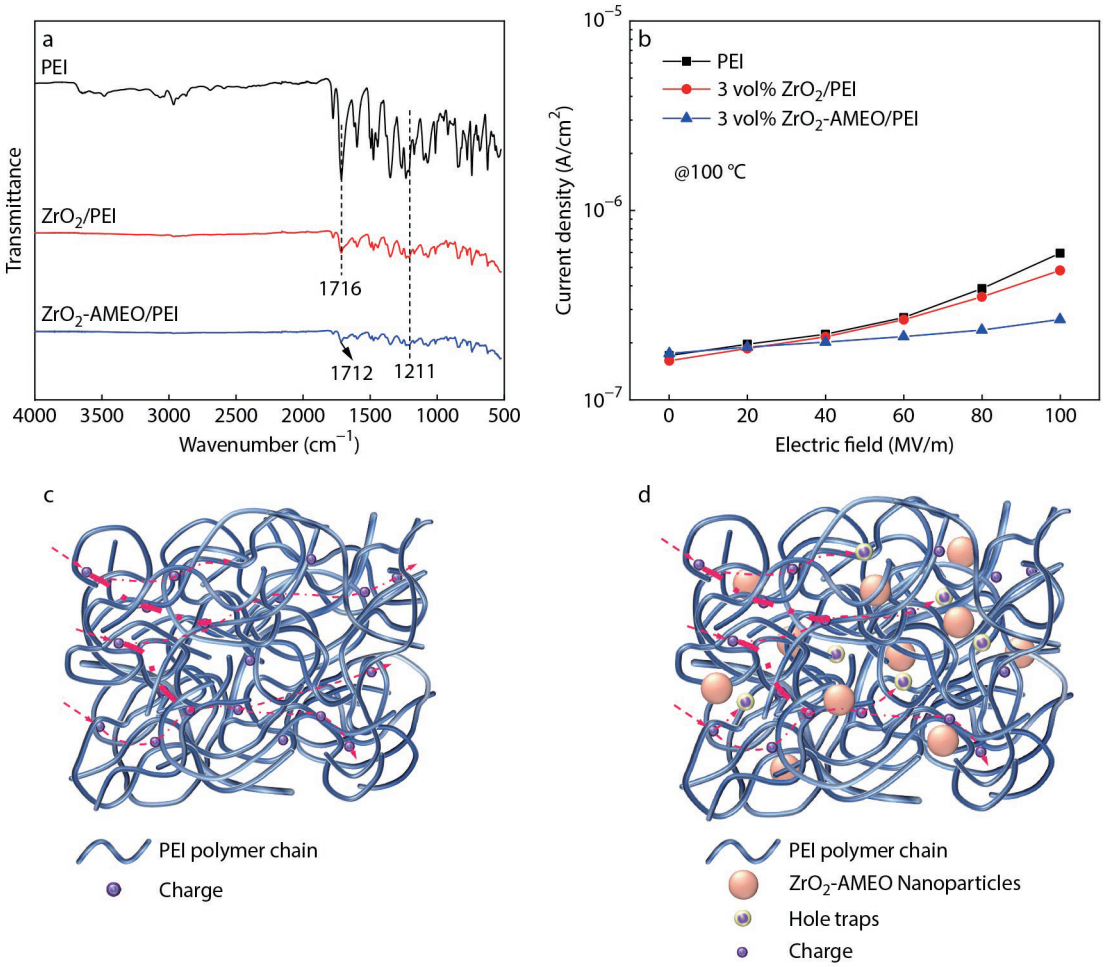

Fig. 10 (a) FTIR spectra of PEI, ZrO_2/PEI and ZrO_2-AMEO/PEI nanocomposites at 4000–500 cm^{-1}; (b) Leakage current for the 3 vol% composites as a function of electric field at 100 °C; Schematic diagram of conduction processes in (c) neat PEI and (d) ZrO_2-AMEO/PEI composite.

within the composites. Therefore, the discharge energy density and high charge-discharge efficiency are improved under high electrical field and high temperature.

Fig. 11 compares the maximum U_d and η of high-temperature dielectric composites at 150 °C with previous reported work.[6,17,19,26,34–41] As seen, the 3 vol% ZrO_2-AMEO/PEI composites achieves a moderate energy density than 3.1 J/cm^3 with 60% efficiency and shows a desirable combination of ultrahigh E_b and η. Combined with the facile preparation, the ZrO_2-AMEO/PEI films suggest great potential for high-temperature energy density capacitor devices.

https://doi.org/10.1007/s10118-024-3068-x

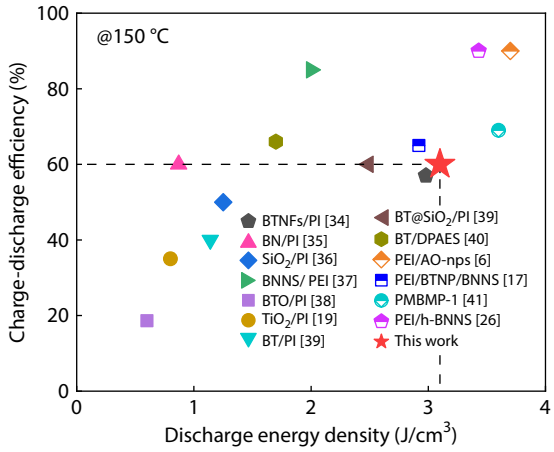

Fig. 11 Comparison of the charge-discharge efficiency at 150 °C between previous reported advanced polymer-based composites and PEI-based composite prepared in this work.

CONCLUSIONS

In this work, ZrO_2 nanoparticles were successfully modified by AMEO and were introduced into the PEI matrix to fabricate PEI-based composites. It has been found that because of the moderate dielectric constant and wide bandgap of ZrO_2 nanoparticles, composites containing ZrO_2 present simultaneous high breakdown strength and improved dielectric constant. Consequently, significant improvements in dielectric properties and energy storage at elevated temperatures can be achieved. Owing to the intrinsic deep trap feature of amino groups in AMEO, the AMEO and ZrO_2 further exhibit coupling effect on suppressing the leakage current both at room temperature and high temperature. The composites containing ZrO_2-AMEO show the maximum discharged energy density of 6.1 J/cm^3 at 25 °C and 3.1 J/cm^3 at 150 °C, which are superior to the commercial BOPP. These results suggest a facile way to enhance the energy storage properties of high-temperature *via* interfacial modification of modest inorganic ceramic with deep trap groups.

Conflict of Interests

The authors declare no interest conflict.

Electronic Supplementary Information

Electronic supplementary information (ESI) is available free of charge in the online version of this article at http://doi.org/10.1007/s10118-024-3068-x.

ACKNOWLEDGMENTS

This work was financially supported by Sichuan Science and Technology Program (No. 2022ZHCG0122), the NSAF project (No. U2230120), Youth Science and Technology Innovation Team of Sichuan Province of Functional Polymer Composites (No. 2021JDTD0009), the Key Researched Development Program of Sichuan Province (No. 2022YFG0271).

REFERENCES

1 Dang, Z.; Yuan, J.; Yao, S.; Liao, R. Flexible nanodielectric materials with high permittivity for power energy storage. *Adv. Mater.* **2013**, *25*, 6334–6365.
2 Hu, P.; Shen, Y.; Guan, Y.; Zhang, X.; Lin, Y.; Zhang, Q.; Nan, C. Topological-structure modulated polymer nanocomposites exhibiting highly enhanced dielectric strength and energy density. *Adv. Funct. Mater.* **2014**, *24*, 3172–3178.
3 Palit, S.; Varghese, D.; Guo, H.; Krishnan, S.; Alam, M. A. The role of dielectric heating and effects of ambient humidity in the electrical breakdown of polymer dielectrics. *IEEE Trans. Device Mat. Rel.* **2015**, *15*, 308–318.
4 Feng, S.; Zhou, Y.; Zhang, T.; Zhang, C; Zhang, Y.; Zhang, Y.; Chen, Q.; Chi, Q. Ultrahigh discharge efficiency and excellent energy density in oriented core-shell nanofiber-polyetherimide composites. *Energy Stor. Mater.* **2020**, *25*, 180–192.
5 Luo, S.; Yu, J.; Yu, S.; Sun, R.; Cao, L.; Liao, W.; Wong, C. Significantly enhanced electrostatic energy storage performance of flexible polymer composites by introducing highly insulating-ferroelectric microhybrids as fillers. *Adv. Energy Mater.* **2019**, *9*, 1803204.
6 Fan, M.; Hu, P.; Dan, Z.; Jiang, J.; Sun, B.; Shen, Y. Significantly increased energy density and discharge efficiency at high temperature in polyetherimide nanocomposites by a small amount of Al_2O_3 nanoparticles. *J. Mater. Chem. A* **2020**, *8*, 24536–24542.
7 Li, H.; Liu, F.; Fan, B.; Ai, D.; Peng, Z.; Wang, Q. Nanostructured ferroelectric-polymer composites for capacitive energy storage. *Small Methods* **2018**, *2*, 1700399.
8 Dang, Z.; Yuan, J.; Zha, J.; Zhou, T.; Li, S.; Hu, G. Fundamentals, processes and applications of high-permittivity polymer-matrix composites. *Prog. Mater. Sci.* **2012**, *57*, 660–723.
9 Rajib, M.; Martinez, R.; Shuvo, M.; Karim, H.; Delfin, D.; Afrin, S.; Rodriguez, G.; Chintalapalle, R.; Lin, Y. Enhanced energy storage of dielectric nanocomposites at elevated temperatures. *Int. J. Appl. Ceram. Technol.* **2016**, *13*, 125–132.
10 Sarlioglu, B.; Morris, C. T. More electric aircraft: review, challenges, and opportunities for commercial transport aircraft. *IEEE Trans. Transp. Electrification* **2015**, *1*, 54–64.
11 Tan, D.; Zhang, L.; Chen, Q.; Irwin, P. High-temperature capacitor polymer films. *J. Electron. Mater.* **2014**, *43*, 4569–4575.
12 Dong, J.; Hu, R.; Xu, X.; Chen, J.; Niu, Y.; Wang, F.; Hao, J.; Wu, K.; Wang, Q.; Wang, H. A facile *in situ* surface-functionalization approach to scalable laminated high-temperature polymer dielectrics with ultrahigh capacitive performance. *Adv. Funct. Mater.* **2021**, *31*, 2102644.
13 Wang, P.; Yao, L.; Pan, Z.; Shi, S.; Yu, J.; Zhou, Y.; Liu, Y.; Liu, J.; Chi, Q.; Zhai, J.; Wang, Q. Ultrahigh energy storage performance of layered polymer nanocomposites over a broad temperature range. *Adv. Mater.* **2021**, *33*, 2103338.
14 Sun, B.; Hu, P.; Ji, X.; Fan, M.; Zhou, L.; Guo, M.; He, S.; Shen, Y. Excellent stability in polyetherimide/SiO_2 nanocomposites with ultrahigh energy density and discharge efficiency at high temperature. *Small* **2022**, *18*, 2202421.
15 Wang, P.; Guo, Y.; Zhou, D.; Li, D.; Pang, L.; Liu, W.; Su, J.; Shi, Z.; Sun, S. High-temperature flexible nanocomposites with ultra-high energy storage density by nanostructured MgO fillers. *Adv. Funct. Mater.* **2022**, *32*, 2204155.
16 Li, Q.; Chen, L.; Gadinski, M. R.; Zhang, S.; Zhang, G.; Li, H. U.; Iagodkine, E.; Haque, A.; Chen, L.; Jackson, T. N.; Wang, Q. Correction: Corrigendum: Flexible high-temperature dielectric materials from polymer nanocomposites. *Nature* **2015**, *523*, 576–579.
17 Li, H.; Ren, L.; Ai, D.; Han, Z.; Liu, Y.; Yao, B.; Wang, Q. Ternary

polymer nanocomposites with concurrently enhanced dielectric constant and breakdown strength for high-temperature electrostatic capacitors. *InfoMat.* **2020**, *2*, 389–400.
18 Liu, F.; Li, Q.; Li, Z.; Liu, Y.; Dong, L.; Xiong, C.; Wang, Q. Poly(methyl methacrylate)/boron nitride nanocomposites with enhanced energy density as high temperature dielectrics. *Compos. Sci. Technol.* **2017**, *142*, 139–144.
19 Ai, D.; Li, H.; Zhou, Y.; Ren, L.; Han, Z.; Yao, B.; Zhou, W.; Zhao, L.; Xu, J.; Wang, Q. Tuning nanofillers in *in situ* prepared polyimide nanocomposites for high-temperature capacitive energy storage. *Adv. Energy Mater.* **2020**, *10*, 1903881.
20 Chen, C.; Xie, Y.; Liu, J.; Li, J.; Wei, X.; Zhang, Z. Enhanced energy storage capability of P(VDF-HFP) nanodielectrics by HfO_2 passivation layer: preparation, performance and simulation. *Compos. Sci. Technol.* **2020**, *188*, 107968.
21 Zheng, W.; Ren, L.; Zhao, X.; Li, H.; Xie, Z.; Li, Y.; Wang, C.; Yu, L.; Yang, L.; Liao, R. Tuning interfacial relaxations in P(VDF-HFP) with Al_2O_3@ZrO_2 core-shell nanofillers for enhanced dielectric and energy storage performance. *Compos. Sci. Technol.* **2022**, *222*, 109379.
22 Ren, L.; Li, H.; Xie, Z.; Ai, D.; Zhou, Y.; Liu, Y.; Zhang, S.; Yang, L.; Zhao, X.; Peng, Z.; Liao, R.; Wang, Q. High-temperature high-energy-density dielectric polymer nanocomposites utilizing inorganic core-shell nanostructured nanofillers. *Adv. Energy Mater.* **2021**, *11*, 2101297.
23 Zhou, Y.; Yuan, C.; Wang, S.; Zhu,Y.; Cheng, S.; Yang, X.; Yang, Y.; Hu, J.; He, J.; Li, Q. Interface-modulated nanocomposites based on polypropylene for high-temperature energy storage. *Energy Stor. Mater.* **2020**, *28*, 255–263.
24 Thakur, Y.; Zhang, T.; Yang, T.; Bernholc, J.; Chen, L. Q.; Runt, J.; Zhang, Q. M. Enhancement of the dielectric response in polymer nanocomposites with low dielectric constant fillers. *Nanoscale* **2017**, *9*, 0992–10997.
25 Zhou, Y.; Wang, Q. Advanced polymer dielectrics for high temperature capacitive energy storage. *J. Appl. Phys.* **2020**, *127*, 240902.
26 Chen, H.; Pan, Z.; Wang, W.; Chen, Y.; Xing, S.; Cheng, Y.; Ding, X.; Liu, J.; Zhai, J.; Yu, J. Ultrahigh discharge efficiency and improved energy density in polymer-based nanocomposite for high-temperature capacitors application. *Compos. Part A Appl. Sci. Manuf.* **2021**, *142*, 106266.
27 Majoul, N.; Aouida, S.; Bessaïs, B. Progress of porous silicon APTES-functionalization by FTIR investigations. *Appl. Surf. Sci.* **2015**, *331*, 388–391.
28 Nakonieczny, D. S.; Kern, F.; Dufner, L.; Dubiel, A.; Antonowicz, M.; Matus, K. Effect of calcination temperature on the phase composition, morphology, and thermal properties of ZrO_2 and Al_2O_3 modified with APTES (3-aminopropyltriethoxysilane). *Materials* **2021**, *14*, 6651.
29 Wang, T.; Li, J.; Niu, F.; Zhong, A.; Liu, J.; Liu, W.; Shan, L.; Zhang, G.; Sun, R.; Wong, C. Low-temperature curable and low-dielectric polyimide nanocomposites using aminoquinoline-functionalized graphene oxide nanosheets. *Compos. B Eng.* **2022**, *228*, 109412.
30 Dai, W.; Yu, J.; Wang, Y.; Song, Y.; Alam, F. E.; Nishimura, K.; Lin, C.; Jiang, N. Enhanced thermal conductivity for polyimide composites with a three-dimensional silicon carbide nanowire@graphene sheets filler. *J. Mater. Chem. A* **2015**, *3*, 4884–4891.
31 Li, X.; Tan, D.; Xie, L.; Sun, H.; Sun, S.; Zhong, G.; Ren, P. Effect of surface property of halloysite on the crystallization behavior of PBAT. *Appl. Clay Sci.* **2018**, *157*, 218–226.
32 Yang, C.; Xie, X.; Lu, Y.; Qi, X.; Lei, Y.; Yang, J.; Wang, Y. Improving the performance of dielectric nanocomposites by utilizing highly conductive rigid core and extremely low loss shell. *J. Phys. Chem. C* **2020**, *124*, 12883–12896.
33 Ren, L.; Yang, L.; Zhang, S.; Li, H.; Zhou, Y.; Ai, D.; Xie, Z.; Zhao, X.; Peng, Z.; Liao, R.; Wang, Q. Largely enhanced dielectric properties of polymer composites with HfO_2 nanoparticles for high-temperature film capacitors. *Compos. Sci. Technol.* **2021**, *201*, 108528.
34 Hu, P.; Sun, W.; Fan, M.; Qian, J.;Jiang, J.; Dan, Z.; Lin, Y.; Nan, C.; Li, M.; Shen, Y. Large energy density at high-temperature and excellent thermal stability in polyimide nanocomposite contained with small loading of $BaTiO_3$ nanofibers. *Appl. Surf. Sci.* **2018**, *458*, 743–750.
35 Cheng, S.; Zhou, Y.; Hu, J.; He, J.; Li, Q. Polyimide films coated by magnetron sputtered boron nitride for high-temperature capacitor dielectrics. *IEEE Trans. Dielectr. Electr. Insul.* **2020**, *27*, 498–503.
36 Zhou,Y.; Li, Q.; Dang, B.; Yang, Y.; Shao, T.; Li, H.; Hu, J.; Zeng, R.; He, J.; Wang, Q. A scalable, high-throughput, and environmentally benign approach to polymer dielectrics exhibiting significantly improved capacitive performance at high temperatures. *Adv. Mater.* **2018**, *30*, 1805672.
37 Azizi, A.; Gadinski, M. R.; Li, Q.; AlSaud, M.; Wang, J.; Wang, Y.; Wang, B.; Liu, F.; Chen, L.; Alem, N.; Wang, Q. High-performance polymers sandwiched with chemical vapor deposited hexagonal boron nitrides as scalable high-temperature dielectric materials. *Adv. Mater.* **2017**, *29*, 1701864.
38 Sun, W.; Lu, X.; Jiang, J.; Zhang, X.; Hu, P.; Li, M.; Lin, Y.; Nan, C.; Shen, Y. Dielectric and energy storage performances of polyimide/$BaTiO_3$ nanocomposites at elevated temperatures. *J. Appl. Phys.* **2017**, *121*, 244101.
39 Dong, J.; Hu, R.; Niu, Y.; Sun, L.; Li, L.; Li, S.; Pan, D.; Xu, X.; Gong, R.; Cheng, J.; Pan, Z.; Wang, Q.; Wang, H. Enhancing high-temperature capacitor performance of polymer nanocomposites by adjusting the energy level structure in the micro-/meso-scopic interface region. *Nano Energy* **2022**, *99*, 107314.
40 Liu, J.; Li, X.; Ma, S.; Zhang, J.; Jiang, Z.; Zhang, Y. Enhanced high-temperature dielectric properties of poly(aryl ether sulfone)/$BaTiO_3$ nanocomposites *via* constructing chemical crosslinked networks. *Macromol. Rapid Commun.* **2020**, *41*, 2000012.
41 Wang, Y.; Li, Z.; Wu, C.; Cao, Y. High-temperature dielectric polymer nanocomposites with interposed montmorillonite nanosheets. *Chem. Eng. J.* **2020**, *401*, 126093.

https://doi.org/10.1007/s10118-024-3068-x